

Article

The Geochemical Characteristics of Source Rock and Oil in the Fukang Sag, Junggar Basin, NW China

Bocai Li ¹, Youjun Tang ¹, Zhonghong Chen ^{1,2}, Yifeng Wang ³, Daxiang He ^{1,*}, Kai Yan ¹ and Lin Chen ⁴

¹ Hubei Key Laboratory of Petroleum Geochemistry and Environment, Yangtze University, Wuhan 430100, China

² School of Geosciences, China University of Petroleum (East China), Qingdao 266580, China

³ PetroChina Research Institute of Petroleum Exploration & Development, Beijing 100083, China

⁴ Exploration and Development Research Institute, Sinopec Shengli Oilfield, Dongying 257001, China

* Correspondence: hedx117@yangtzeu.edu.cn

Abstract: The Fukang Sag in the Junggar Basin is the main exploration block. However, the origin and source of crude oil are still controversial, which seriously affects the well locating and exploration in this area. In the present work, 30 source rocks and 21 crude oils were collected for geochemical analysis to clarify the source of the organic matter, the sedimentary environment, and the evolution degree. Among them, the source rocks of the Pingdiquan Formation are type II₁ organic matter with good quality, the source rocks of the Badaowan Formation are type II₂-III organic matter with fair–good quality, and the source rocks of the Xishanyao Formation are type II₂ organic matter with fair quality. All source rocks are in the mature stage. The results of the biomarker compounds show that the lacustrine mudstone of the Xishanyao Formation and the coal-measure mudstone of the Badaowan Formation were deposited in reducing environments. The former was mainly from lower aquatic organisms, and the latter was from terrestrial higher plants. The mudstone of the Pingdiquan Formation was formed in a weakly oxidizing–weakly reducing depositional environment, and its parent material was of mixed origin. Based on the results of the biomarker compounds and carbon isotopes, the crude oils were divided into three categories. The Family I crude oil has the characteristics of low maturity, low salinity, and more input of low-level aquatic organisms, and the carbon isotope has a good affinity with the lacustrine mudstone of the Xishanyao Formation. The Family II crude oil shows medium maturity, low salinity, mainly higher plant input, and heavy carbon isotope, mainly derived from the Badaowan Formation coal-measure mudstone. The Family III crude oil is characterized by high maturity, high salinity, mixed parent materials, and light carbon isotope and originates from the mudstone of the Pingdiquan Formation. The results provide a reference for oil and gas exploration and development in the eastern area of the Junggar Basin; the future research will focus on well areas with high maturity near the Fukang fault zone.

Keywords: oil family; biomarkers; carbon isotope; Fukang Sag; Junggar basin



Citation: Li, B.; Tang, Y.; Chen, Z.; Wang, Y.; He, D.; Yan, K.; Chen, L. The Geochemical Characteristics of Source Rock and Oil in the Fukang Sag, Junggar Basin, NW China. *Minerals* **2023**, *13*, 432. <https://doi.org/10.3390/min13030432>

Academic Editors: Mahmoud Leila, Yubin Bai, Bojiang Fan and Thomas Gentzis

Received: 11 February 2023

Revised: 8 March 2023

Accepted: 16 March 2023

Published: 17 March 2023



Copyright: © 2023 by the authors. Licensee MDPI, Basel, Switzerland. This article is an open access article distributed under the terms and conditions of the Creative Commons Attribution (CC BY) license (<https://creativecommons.org/licenses/by/4.0/>).

1. Introduction

In the long process of geological evolution, oil and gas undergo a series of secondary changes in migration, enrichment, and evolution, resulting in changes in the oil and gas properties [1–4]. However, geological and geochemical methods can be used to study the relationship between the oil and gas and the source rocks [5–7]. Commonly used oil source comparison parameters include alkane, cycloalkanes, stable carbon isotopes, and biomarkers [8–11]. Based on biomarkers and hydrocarbon fraction carbon isotopes, researchers have evaluated the organic matter input and evolution [12–16]. In recent years, rich achievements have been made in hydrocarbon exploration in the Junggar Basin. Hydrocarbon-rich sags such as Mahu, Shawan, and Sikeshu have overcome breakthroughs, opening a new chapter in oil and gas exploration in the western sag of the basin [17–21]. In

the Baijiahai bulge, North Santai bulge, Fukang fault zone, and other tectonic units around the Fukang Sag, North Santai, Santai, Ganhe, Cainan, Shanan, and Shabei oil fields have been discovered, confirming that the area has good exploration potential [22,23]. Due to the development of multiple sets of hydrocarbon source rocks and the adjustment and transformation of oil reservoirs, the classification and genesis of the crude oil have become a hot spot. [24–27]. Previous researchers have put forward different views on the types and genesis of crude oil in Fukang Sag and its surroundings. Some scholars believe that the crude oil mainly comes from multiple sets of hydrocarbon source rocks from the Permian Pingdiquan Formation [28,29]. Other scholars believe that there are other hydrocarbon source rocks, such as Carboniferous, Permian, Triassic, and Jurassic hydrocarbon source rocks [30–32]. These disputes seriously restrict the development and breakthrough of oil and gas deployment in Fukang Sag.

This work aimed to strengthen the understanding of the organic geochemical characteristics, the sources of the organic matter, and the sedimentary environment of the Jurassic rocks and oils in Fukang Sag. Furthermore, the oil's genetic families and oil source correlation were summarized. The present study is conducive to expanding the scale of oil and gas exploration in the eastern part of the Junggar Basin, thus balancing regional development differences and playing an important theoretical role in future oil and gas deployment and development.

2. Geological Setting

Junggar Basin is an inland basin located in North Tianshan Mountain, sandwiched between Zaire, Qinggelidi Mountain, and Kelameili Mountain [33,34]. Fukang Sag extends along $44^{\circ}10'–44^{\circ}30' N$ and $87^{\circ}30'–88^{\circ}40' E$, belonging to the Changji Hui Autonomous Prefecture (Figure 1a). In terms of its structural position, it belongs to the slope belt of the central depression, which is adjacent to the Baijiahai bulge and the Fukang fault zone. [23,35–37] (Figure 1b). The target layer is deeply buried, and the structural form is relatively simple, but the structural evolution and burial history are relatively complex.

With a basement of the Hercynian fold in the tectonic development and evolution of the Junggar basin [38], Fukang Sag has experienced three major tectonic movements: the late Hercynian movement, the Indochina movement, and the Yanshan movement. According to the regional geological data, unconformity data, and sedimentary evolution characteristics, the basin can be divided into three tectonic evolution stages, namely, the late Carboniferous–Permian collision foreland basin stage, the Triassic–Paleogene inland depression basin stage, and the Neogene–Quaternary regeneration foreland basin stage [23,39].

The Jurassic system can be further divided into the Lower Jurassic Badaowan Formation and the Sangonghe Formation, the Middle Jurassic Xishanyao Formation and Toutunhe Formation, and the Upper Jurassic Qigu Formation and Kalazha Formation. The main exploration targets of the study block are the Badaowan Formation and the Xishanyao Formation of the Jurassic System [40]. In addition, the Badaowan Formation is a coal-bearing formation, and the middle part is coal-measure mudstone mixed with thin coal. The Xishanyao Formation is a lacustrine coal measure stratum, which is mainly interbedded with mudstone and sandstone and interbedded with gray–black carbonaceous mudstone (Figure 2).

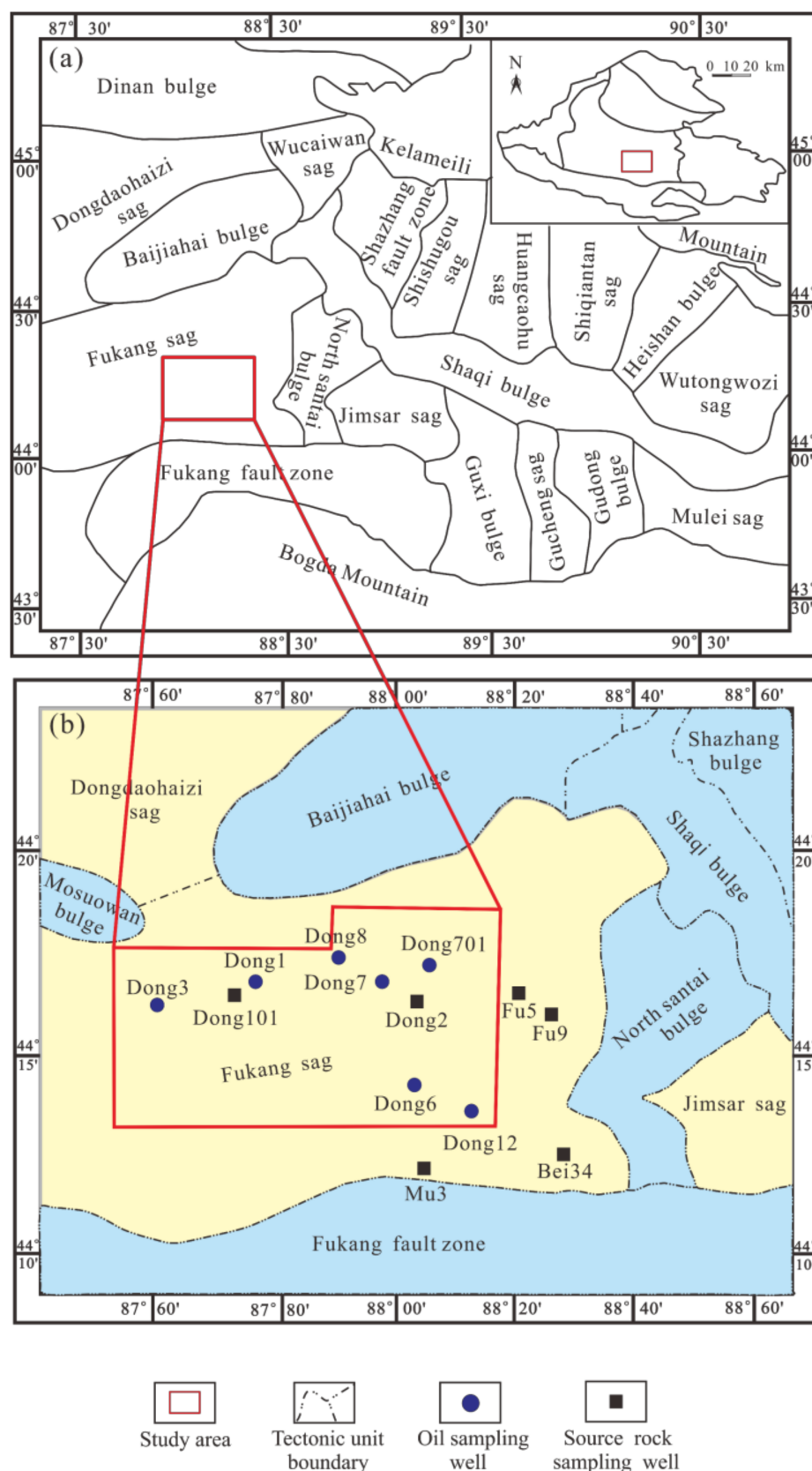


Figure 1. Study area location (a), sampling point in Fukang Sag (b).

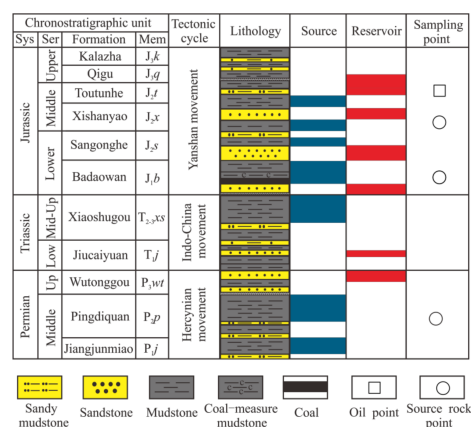


Figure 2. Stratigraphic column of the Permian–Jurassic system in Fukang Sag.

3. Materials and Methods

3.1. Samples

The samples were collected from Dong 1, Dong 101, Dong 2, Dong 3, Dong 7, Dong 701, Dong 8, Fu5, Fu9, Mu3, and Bei 34 in the Fukang Sag, including 30 source rocks and 21 crude oils. The source rock collection horizon was concentrated in the Pingdiquan Formation, Badaowan Formation, and Xishanyao Formation, and the crude oil collection horizon was in the Toutunhe Formation (Figure 2). Bitumen chloroform “A” was obtained by Soxhlet extraction for 72 h. After n-hexane precipitation and filtration of the asphaltene, the group components were separated by filling the solid-phase chromatography column. The saturated hydrocarbon, aromatic hydrocarbon, and nonhydrocarbon components were obtained by adding n-hexane, n-hexane, and dichloromethane mixed solvent and dichloromethane and methanol mixed solvent, successively.

3.2. Total Organic Carbon (TOC) and Rock-Eval Pyrolysis

A LECO CS230 carbon–sulfur analyzer (Beijing, China) was used for TOC analysis following the Chinese National Standard GB/T19145-2003 [41]. Before the experiments, the rock samples were crushed and passed through a 0.08 mm sieve. After drying at a low temperature, the samples were weighed, and 80~120 mg was added into a crucible; then, we added dilute hydrochloric acid into the section of the inorganic carbon reaction, and the total organic carbon test was carried out after the removal of the inorganic carbon.

The rock samples from 6 wells were tested with a Vinci Technologies Rock-Eval analyzer for pyrolysis analysis following the Chinese National Standard GB/T 18602-2012 [42]. The derived parameters of pyrolysis included S₁ (keep the temperature at 300 °C for 3 min) and S₂ (oven temperature increase to 600 °C at intervals of 50 °C/min).

3.3. Gas Chromatography (GC) and Gas Chromatography–Mass Spectrometry (GC-MS)

An Agilent 7890 gas chromatographer was used for the saturated hydrocarbon GC analysis; these analyses were carried out with a procedure similar to that of Li et al. [43]. The initial GC oven temperature was 50 °C, remaining for 1 min; then, the temperature was increased from 50 °C to 100 °C at intervals of 20 °C/min. Then, we increased the temperature from 100 °C to 315 °C at intervals of 3 °C/min, remaining for 16 min. The sample inlet temperature was 300 °C, the carrier gas was helium, the flow rate was 1.0 mL/min, the scanning range was 50~550 AMU, the detection mode was full scan detection, and the ionization energy was 70 eV.

3.4. Stable Carbon Isotope Analysis

The stable carbon isotope ratio was analyzed by an HP6980 mass spectrometer following the Chinese National Standard GB/T 183402-2010 [42]. The temperature was raised

from 80 °C to 300 °C at intervals of 4 °C/min for 20 min. All stable isotope values were the average of at least 3 tests and expressed as δ according to the V-PDB standard.

4. Results

4.1. Geochemical Characteristics of Crude Oils

4.1.1. Characteristics of n-Alkanes and Isoprenoids

The extracts of the Dong1 and Dong3 crude oil had relatively high $C_{19+20}/C_{19+20+21+23}$ values, which were 0.62–0.70 (avg. 0.65). Moreover, they had the highest Pr/Ph ratio of any crude, ranging from 2.95 to 3.05 (avg. 3.00), which showed pristane predominance (Table 1). The obvious C_{24} tetracyclic terpane advantage resulted in $C_{24}TeT/C_{26}TT$ ratios, which ranged from 3.50 to 4.60 (avg. 4.05). The Dong7, Dong701, and Dong8 crude oil $C_{19+20}/C_{19+20+21+23}$ ratios were relatively low and varied from 0.44 to 0.53 (avg. 0.48). The ratio values of the Pr/Ph were distributed from 2.05 to 2.34, with an average of 2.16, which showed a distinct pristane advantage. The ratios of the $C_{24}TeT/C_{26}TT$ were slightly lower than that of the former, which were mainly distributed between 2.1 to 2.8 (avg. 2.44). Significantly different from the previous crude oil, the $C_{19+20}/C_{19+20+21+23}$ ratios, Pr/Ph ratios, and $C_{24}TeT/C_{26}TT$ ratios of the Dong 6 and Dong 12 were the lowest, and their distribution ranges were 0.33–0.38 (avg. 0.36), 1.80–1.89 (avg. 1.85), and 1.53–1.81 (avg. 1.69), respectively.

Table 1. Biomarker characteristics of the source rocks and crude oil samples in Fukang Sag.

Sample	Formation	Type	1	2	3	4	5	6	7	8	9	10	11
Dong101-1	J ₁ b	source rock	0.77	3.33	4.40	17%	25%	58%	0.23	0.06	0.54	0.56	0.49
Dong101-2	J ₁ b	source rock	0.72	3.22	4.20	15%	22%	63%	0.25	0.10	0.52	0.52	0.51
Dong101-3	J ₁ b	source rock	0.73	3.09	4.17	13%	31%	56%	0.25	0.09	0.55	0.52	0.50
Dong101-4	J ₁ b	source rock	0.82	3.11	4.52	15%	27%	58%	0.21	0.08	0.53	0.53	0.50
Dong101-5	J ₁ b	source rock	0.88	3.29	4.55	14%	30%	56%	0.20	0.09	0.55	0.55	0.51
Dong101-6	J ₁ b	source rock	0.79	3.18	4.38	15%	27%	58%	0.23	0.06	0.55	0.54	0.51
Dong2-1	J ₂ x	source rock	0.45	2.01	2.50	38%	23%	39%	0.91	0.10	0.38	0.50	0.40
Dong2-2	J ₂ x	source rock	0.42	1.99	2.45	35%	27%	38%	0.87	0.12	0.37	0.45	0.42
Dong2-3	J ₂ x	source rock	0.47	2.07	2.37	33%	27%	40%	0.84	0.12	0.35	0.47	0.42
Dong2-4	J ₂ x	source rock	0.45	2.03	2.98	37%	25%	38%	0.88	0.14	0.35	0.45	0.41
Dong2-5	J ₂ x	source rock	0.43	2.11	2.22	35%	25%	40%	0.89	0.15	0.37	0.45	0.40
Fu9	J ₂ x	source rock	0.43	2.11	2.30	39%	25%	36%	0.97	0.18	0.38	0.43	0.42
Fu5-1	P ₂ p	source rock	0.33	1.49	1.35	42%	29%	29%	0.55	0.42	0.65	0.62	0.52
Fu5-2	P ₂ p	source rock	0.32	1.47	1.32	41%	32%	27%	0.52	0.38	0.71	0.61	0.54
Mu3-1	P ₂ p	source rock	0.37	1.52	1.21	40%	27%	33%	0.49	0.21	0.69	0.59	0.49
Mu3-2	P ₂ p	source rock	0.35	1.52	1.11	39%	26%	35%	0.47	0.23	0.64	0.57	0.51
Mu3-3	P ₂ p	source rock	0.32	1.55	1.03	40%	25%	35%	0.59	0.27	0.66	0.56	0.50
Bei34	P ₂ p	source rock	0.39	1.57	1.44	40%	27%	33%	0.64	0.38	0.63	0.65	0.54
Dong1-1	J ₂ t	crude oil	0.63	3.05	3.50	15%	25%	60%	0.25	0.05	0.45	0.53	0.50
Dong1-2	J ₂ t	crude oil	0.62	2.98	3.90	12%	24%	64%	0.19	0.08	0.48	0.55	0.49
Dong3-1	J ₂ t	crude oil	0.70	3.01	4.20	19%	25%	56%	0.28	0.06	0.50	0.52	0.48
Dong3-2	J ₂ t	crude oil	0.65	2.95	4.60	16%	26%	58%	0.34	0.06	0.47	0.52	0.50
Dong7-1	J ₂ t	crude oil	0.51	2.18	2.20	42%	20%	38%	1.11	0.14	0.39	0.47	0.35
Dong7-2	J ₂ t	crude oil	0.53	2.19	2.30	45%	22%	33%	1.36	0.13	0.38	0.45	0.42
Dong7-3	J ₂ t	crude oil	0.49	2.11	2.30	43%	23%	34%	1.26	0.17	0.37	0.47	0.42
Dong7-4	J ₂ t	crude oil	0.45	2.11	2.40	41%	23%	36%	1.14	0.16	0.33	0.48	0.40
Dong7-5	J ₂ t	crude oil	0.48	2.12	2.40	39%	21%	40%	0.98	0.16	0.38	0.50	0.42
Dong7-6	J ₂ t	crude oil	0.50	2.11	2.60	41%	22%	37%	1.11	0.15	0.32	0.51	0.41
Dong701-1	J ₂ t	crude oil	0.45	2.34	2.50	42%	22%	36%	1.17	0.11	0.37	0.49	0.37
Dong701-2	J ₂ t	crude oil	0.48	2.23	2.80	43%	20%	37%	1.16	0.16	0.35	0.55	0.39
Dong701-3	J ₂ t	crude oil	0.42	2.13	2.90	36%	25%	39%	0.92	0.11	0.36	0.43	0.41
Dong701-4	J ₂ t	crude oil	0.44	2.16	2.10	40%	20%	40%	1.00	0.17	0.39	0.43	0.43
Dong8-1	J ₂ t	crude oil	0.47	2.17	2.40	32%	21%	48%	0.67	0.15	0.35	0.39	0.42
Dong8-2	J ₂ t	crude oil	0.49	2.05	2.20	38%	22%	40%	0.95	0.15	0.36	0.40	0.41
Dong8-3	J ₂ t	crude oil	0.50	2.20	2.60	38%	21%	41%	0.93	0.17	0.38	0.40	0.42
Dong6-1	J ₂ t	crude oil	0.38	1.82	1.80	35%	20%	45%	0.78	0.25	0.62	0.59	0.52
Dong6-2	J ₂ t	crude oil	0.35	1.89	1.81	37%	25%	38%	0.80	0.26	0.60	0.55	0.54
Dong12-1	J ₂ t	crude oil	0.33	1.80	1.53	33%	25%	42%	0.88	0.29	0.59	0.57	0.54
Dong12-2	J ₂ t	crude oil	0.37	1.88	1.60	37%	22%	41%	0.97	0.23	0.59	0.55	0.55

1: $C_{19+20}/C_{19+20+21+23}$; 2: Pr/Ph: pristane/phytane; 3: $C_{24}TeT/C_{26}TT$: C_{24} tetracyclic terpane/ C_{26} tricyclic terpane; 4: $C_{27}/\sum C_{27-29}$ regular steranes; 5: $C_{28}/\sum C_{27-29}$ regular steranes; 6: $C_{29}/\sum C_{27-29}$ regular steranes; 7: C_{27}/C_{29} regular steranes; 8: Ga/ $C_{30}H$: gammacerane/ C_{30} hopane; 9: Ts/(Ts + Tm):18 α -22,29,30-trisnorneohopane/(18 α -22,29,30-trisnorneohopane+17 α -22,29,30-trisnorhopane); 10: C_{29} -sterane $\beta\beta/(\alpha\alpha + \beta\beta)$; 11: $\alpha\alpha$ C_{29} -sterane 20S/(20S + 20R).

4.1.2. Characteristics of Steranes and Hopanes

The oils of Dong1 and Dong3 had relatively high $\alpha\alpha\alpha\text{C}_{29}$ -sterane $20\text{S}/(20\text{S} + 20\text{R})$ and C_{29} -sterane $\beta\beta/(\alpha\alpha + \beta\beta)$ ratios, which were 0.48–0.50 (avg. 0.49) and 0.52–0.55 (avg. 0.53), respectively. In this study, the T_s contents were lower than the T_m , and the $T_s/(T_s + T_m)$ ratios varied between 0.45 and 0.50 (avg. 0.48), which were at a moderate level (Table 1). The $\alpha\alpha\alpha 20\text{RC}_{27}\text{-C}_{28}\text{-C}_{29}$ regular sterane distribution patterns of the oil samples were “Inverted L”-shaped (Figure 3). The relative contents of the C_{27} regular sterane were lower than those of the C_{29} regular sterane, and the $\text{C}_{27}/\text{C}_{29}$ ratios ranged from 0.19 to 0.34 (avg. 0.26). The gammacerane/ C_{30} -hopane were relatively low and varied from 0.05 to 0.08 (avg. 0.06). The oils of Dong7, Dong701, and Dong8 had the relatively lowest $\alpha\alpha\alpha\text{C}_{29}$ -sterane $20\text{S}/(20\text{S} + 20\text{R})$ and C_{29} -sterane $\beta\beta/(\alpha\alpha + \beta\beta)$ ratios, which were 0.35–0.43 (avg. 0.41) and 0.39–0.55 (avg. 0.46), respectively, which reflected that these oil samples had low maturity. The ratios of the $T_s/(T_s + T_m)$ were lower than 0.4, ranging from 0.32 to 0.39 (avg. 0.36). In the relative content of the regular steranes, the content of the regular steranes of C_{27} and C_{29} was similar, the peak pattern was mainly “V”-shaped (Figure 3), and the ratios of $\text{C}_{27}/\text{C}_{29}$ were concentrated in 0.92–1.36 (avg. 1.06). The ratios of gammacerane/ C_{30} -hopane were higher than the former, varying between 0.11 and 0.17 (avg. 0.15). Obviously different from the other crude oils, Dong 6 and Dong 12 had the highest $\alpha\alpha\alpha\text{C}_{29}$ -sterane $20\text{S}/(20\text{S} + 20\text{R})$, C_{29} -sterane $\beta\beta/(\alpha\alpha + \beta\beta)$ ratios, and $T_s/(T_s + T_m)$ ratios, which ranged from 0.52 to 0.54 (avg. 0.54), 0.55 to 0.59 (avg. 0.57), and 0.59 to 0.62 (avg. 0.60), respectively. The $\alpha\alpha\alpha 20\text{RC}_{27}\text{-C}_{28}\text{-C}_{29}$ regular sterane distribution patterns of the oil samples were “L”-shaped (Figure 3). The relative contents of the C_{27} regular sterane were slightly lower than those of the C_{29} regular sterane, and the $\text{C}_{27}/\text{C}_{29}$ ratios ranged from 0.78 to 0.97 (avg. 0.86). The ratios of the gammacerane/ C_{30} -hopane were the highest, varying from 0.23 to 0.29 (avg. 0.26).

4.2. Geochemical Characteristics of the Source Rocks

4.2.1. Characteristics of the Coal-Measure Mudstone of the Badaowan Formation

The TOC content, $S_1 + S_2$, of the coal-measure mudstone of the Badaowan Formation ranged from 2.47% to 3.14% (avg. 2.83%) and 2.04 to 2.61 mg/g (avg. 2.31 mg/g), respectively (Figure 4a and Table 2). As shown in Figure 4a, the rock samples were identified as fair to good source rocks [44,45]. The value of the Hydrogen Index (HI) and the T_{max} from the coal-measure mudstone ranged between 104.24 and 133.11 mg/g (avg. 117.71 mg/g) and between 439 and 449 °C, with a mean value of 442 °C, respectively. The low HI value reflected the existence of a large number of terrigenous plants in the parent source [46]. In addition, in the combined HI versus T_{max} kerogen type classification diagrams, the Badaowan Formation rock samples represented type II₂-III kerogen (Figure 4b) [47,48].

Table 2. The geochemical characteristics of the source rocks in Fukang Sag.

Formation	TOC/%	$S_1 + S_2$ (mg/g)	Hydrogen Index (mg/g)	T_{max} (°C)	Organic Matter Type	Abundance Evaluation
P _{2p}	3.33–4.86 4.16(10)	4.04–5.55 4.73(10)	223.12–259.73 241.29(10)	446–455 450(10)	II ₁	Good
J _{1b}	2.47–3.14 2.83(10)	2.04–2.61 2.31(10)	104.24–133.11 117.71(10)	439–449 442(10)	II ₂ -III	Fair-Good
J _{2x}	1.85–2.43 2.11(10)	1.74–2.17 2.01(10)	156.25–198.52 174.78(10)	432–441 438(10)	II ₂	Fair

Note: Min~Max; Avg (Number).

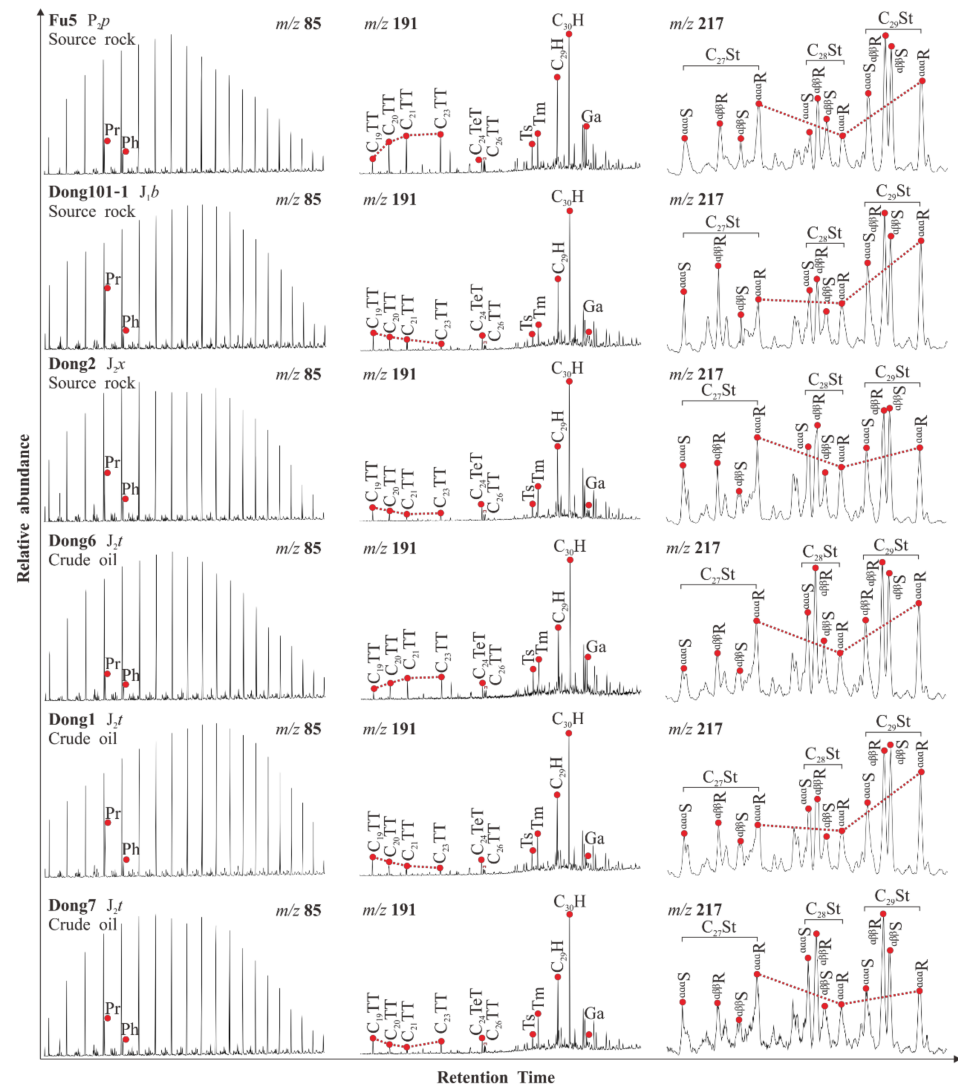


Figure 3. The GC-MS characteristics of the saturated hydrocarbon of the typical source rock and crude oil in Fukang Sag.

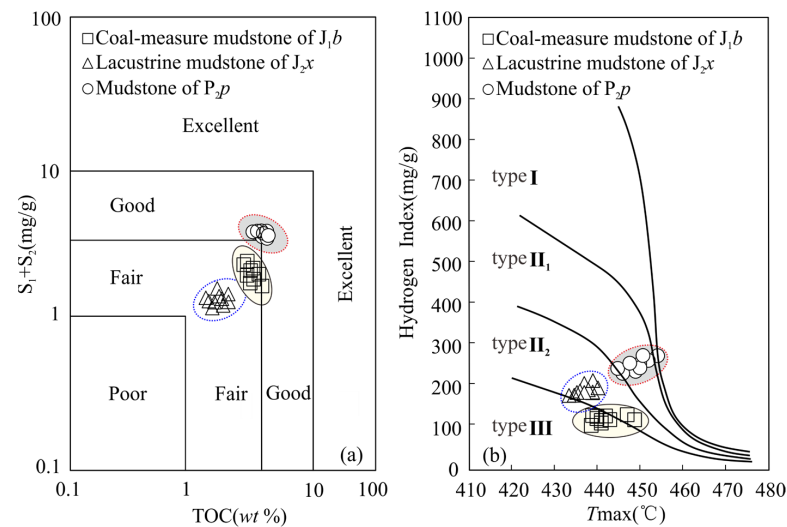


Figure 4. The TOC versus $S_1 + S_2$ of samples in the Fukang Sag (a), T_{max} versus Hydrogen Index showing the types of kerogen (b).

The $C_{19+20}/C_{19+20+21+23}$ ratios can be used to determine the origin of organic matter [49,50]. Generally, terrestrial organic matter has high $C_{19+20}/C_{19+20+21+23}$ ratios, while marine organic matter has low ratios [51–53]. The $C_{19+20}/C_{19+20+21+23}$ ratio of the coal-measure mudstone of the Badaowan Formation was relatively high, with a distribution range of 0.72–0.88 and an average value of 0.79, indicating that the terrigenous plants were significant. (Table 1). The ratio of pristane/phytane (Pr/Ph) is a vital parameter and is widely used to indicate sedimentary environments and sources of organic matter [54,55]. The consensus is that low Pr/Ph (Pr/Ph < 1) reflects the depositional environment of reduction, moderate Pr/Ph ($1 \leq \text{Pr/Ph} < 3$) reveals a transitional sedimentary environment, and high Pr/Ph (Pr/Ph > 3) represents an oxidized terrigenous sedimentary environment [12,56]. The high Pr/Ph (3.09–3.33) ratios reflect the pristane predominance of the Badaowan Formation coal-measure mudstones (Table 1), and they were mainly derived from a terrestrial sedimentary environment in a low-salinity oxidation environment. $C_{24}\text{TeT}$ occupied a large proportion in the terrestrial parent material [57–59], and the distribution range of the $C_{24}\text{TeT}/C_{26}\text{TT}$ ratios of the Badaowan Formation were 4.17–4.55 (avg. 4.37), which was important evidence of the source of terrestrial matter. The C_{27} and C_{28} regular steranes were derived from marine organic algae and lake algae, respectively, while the C_{29} regular steranes were derived from terrestrial higher plants. Therefore, the relative abundance of $\alpha\alpha\alpha 20\text{RC}_{27-29}$ of regular steranes is often used to distinguish organic matter types [60]. The relative contents of C_{27} (13%–17%) were obviously lower than C_{29} (56%–63%), and the C_{27}/C_{29} was concentrated at 0.20–0.25 (avg. 0.23), proving terrestrial higher plants were the main parent material. As an indicator of the deposition environment, the gammacerane indicates a strong reduction and high salinity deposition environment when a high value occurs, and there will be a certain water stratification phenomenon in the water [56,61]. The Badaowan Formation mudstone samples had low gammacerane contents, and only sample Dong101-2 had a gammacerane to C_{30} hopane ratio of 0.10, indicating the sedimentary water body was fresh water.

The ratios of the C_{29} steranes isomers can reflect the maturity of the source rocks, and $\alpha\alpha\alpha C_{29}$ -sterane $20\text{S}/(20\text{S} + 20\text{R})$ and C_{29} -sterane $\beta\beta/(\alpha\alpha + \beta\beta)$ are considered valid indicators of maturity [57]. The values of the $\alpha\alpha\alpha C_{29}$ -sterane $20\text{S}/(20\text{S} + 20\text{R})$ and C_{29} -sterane $\beta\beta/(\alpha\alpha + \beta\beta)$ were 0.49–0.51 (avg. 0.50) and 0.52–0.56 (avg. 0.54), respectively, which were relatively high (Table 1). Furthermore, $T_s/(T_s + T_m)$ is a common parameter and increases with increasing maturity; the ratios of $T_s/(T_s + T_m)$ varied from 0.52 to 0.55 (avg. 0.54), indicating jointly that the coal-measure mudstones reached the mature stage.

4.2.2. Characteristics of the Lacustrine Mudstone of the Xishanyao Formation

The TOC, $S_1 + S_2$, Hydrogen Index (HI), and T_{max} values of the lacustrine mudstone of the Xishanyao Formation ranged from 1.85% to 2.43% (avg. 2.11%), 1.74 to 2.17 mg/g (avg. 2.01 mg/g), 156.25 to 198.52 mg/g (avg. 174.78 mg/g), and 432 to 441 °C, with a mean value of 438 °C, respectively (Table 2). In general, the lacustrine mudstone was type II₂ kerogen, which reached the mature stage and had a moderate hydrocarbon generation capacity; so, it was a medium source rock (Figure 4).

The extracts of the Xishanyao Formation lacustrine mudstones had medium $C_{19+20}/C_{19+20+21+23}$ ratios, which ranged from 0.42 to 0.47 (avg. 0.44). In addition, the $C_{24}\text{TeT}/C_{26}\text{TT}$ ratios of the samples were relatively medium varying from 2.22 to 2.98 (avg. 2.47), which reflected the input characteristics of terrestrial higher plants and algae. The relative percentages of the C_{27} and C_{29} were approximately the same, which were located at 33%–39% and 36%–40%, respectively (Table 1). To a large extent, it proved that the parent source had the characteristics of mixed sources. The gammacerane/ C_{30} -hopane of the lacustrine mudstone of the Xishanyao Formation varied between 0.10 and 0.18, with an average of 0.14, indicating the sedimentary water body was fresh water, the water body was shallow, and there was no obvious stratification. The Xishanyao Formation samples had relatively low $\alpha\alpha\alpha C_{29}$ -sterane $20\text{S}/(20\text{S} + 20\text{R})$ and C_{29} -sterane $\beta\beta/(\alpha\alpha + \beta\beta)$ ratios, which varied from 0.40 to 0.42 (avg. 0.41) and 0.43 to 0.50 (avg. 0.46), respectively. They showed relatively

low $T_s/(T_s+T_m)$ ratios at 0.37, identifying the maturity was far lower than other numbers, and it was in the low mature evolutionary stage.

4.2.3. Characteristics of the Mudstone of the Pingdiquan Formation

The mudstone of the Pingdiquan Formation had a higher total organic carbon content, ranging from 3.33 to 4.86% (avg. 4.16%) (Figure 4a; Table 2). The HI values were between 223.12 and 259.73 mg/g (avg. 241.29 mg/g). The type of organic matter was II₁ (Figure 4b). The T_{max} values and $S_1 + S_2$ (avg. 4.73 mg/g) indicated that the organic matter reached the mature stage and belonged to the category of good source rocks.

The relatively low $C_{19+20}/C_{19+20+21+23}$ ratios of the Pingdiquan Formation mudstone samples ranged between 0.32 and 0.39, with an average of 0.35, also supporting the marine organic matter source. The Pr/Ph of the mudstone of the Pingdiquan Formation varied between 1.47 and 1.57 (avg. 1.52), indicating the mudstone mainly came from the weak oxidation–weak reduction marine sedimentary environment. Moreover, the low $C_{24}TeT/C_{26}TT$ ratios ranging from 1.03 to 1.44 could be indicative of algae organic matter inputs. In this study, the relative contents of C_{27} (39%–42%) were obviously higher than the C_{29} (27%–35%), and the C_{27}/C_{29} was concentrated at 0.47–0.64 (avg. 0.54). A certain amount of gammacerane was detected in the mudstone of the Pingdiquan Formation, whose ratios ranged from 0.21 to 0.42 (avg. 0.32), indicating the mudstone was deposited in a brackish marine environment. The Pingdiquan Formation mudstone samples had relatively high $\alpha\alpha\alpha C_{29}$ -sterane $20S/(20S + 20R)$ and C_{29} -sterane $\beta\beta/(\alpha\alpha + \beta\beta)$ ratios (Table 1), which varied from 0.49 to 0.54 (avg. 0.52) and 0.56 to 0.65 (avg. 0.60), respectively. They showed relatively high $T_s/(T_s + T_m)$ ratios varying from 0.63 to 0.71 (avg. 0.66), showing the samples reached a higher stage of thermal evolution.

5. Discussion

5.1. Oil Family Classification

The Family I oil mainly included Dong7, Dong701, and Dong8; the ratios of the $C_{19+20}/C_{19+20+21+23}$ and $C_{24}TeT/C_{26}TT$ were slightly lower than those of the other ethnic groups and at a medium level. The C_{27}/C_{29} indicated that in the parent source, it was mainly algae input. The results of the Pr/Ph and gammacerane/ C_{30} -hopane showed the oil samples were deposited in a lacustrine sedimentary environment with weak oxidation and weak reduction [56]. The isomerization index of steranes indicated an early mature stage with low maturity.

The Family II oil was located in Dong1 and Dong3, which had high $C_{19+20}/C_{19+20+21+23}$ and $C_{24}TeT/C_{26}TT$ ratios and low C_{27}/C_{29} ratios, indicating that the oils were derived from terrestrial higher plants (Figure 5). The results of the Pr/Ph and gammacerane/ C_{30} -hopane suggested that the oil samples were deposited in a fresh environment with low salinity. On the $\alpha\alpha\alpha C_{29}$ -sterane $20S/(20S + 20R)$ versus C_{29} -sterane $\beta\beta/(\alpha\alpha + \beta\beta)$ cross plot, all of the Family II oil samples showed a mature stage.

The Family III oil was located in Dong6 and Dong12; the $C_{19+20}/C_{19+20+21+23}$, $C_{24}TeT/C_{26}TT$, and $\alpha\alpha\alpha C_{29}$ relative contents of the Family III oil showed that the samples of organic matter were mainly a mixture of algae and terrestrial higher plants (Figure 5), and its high gammacerane/ C_{30} -hopane value suggested a saltwater environment with high salinity (Figure 6a). Compared with other crude oil samples, it had the highest maturity and reached the mature stage of thermal evolution (Figure 6b).

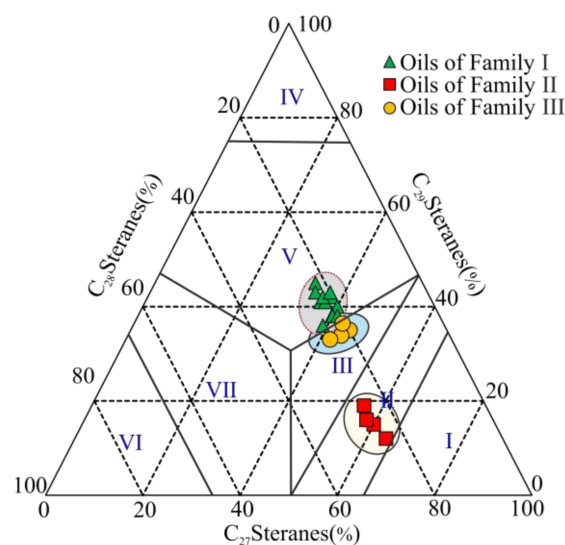


Figure 5. C_{27} , C_{28} , and C_{29} show the origin of organic matter in oil samples. (I: Terrestrial plant, II: Mainly terrestrial plant, III: Mixed source, IV: Phycophyta, V: Mainly Phycophyta, VI: Plankton, VII: Mainly Plankton.).

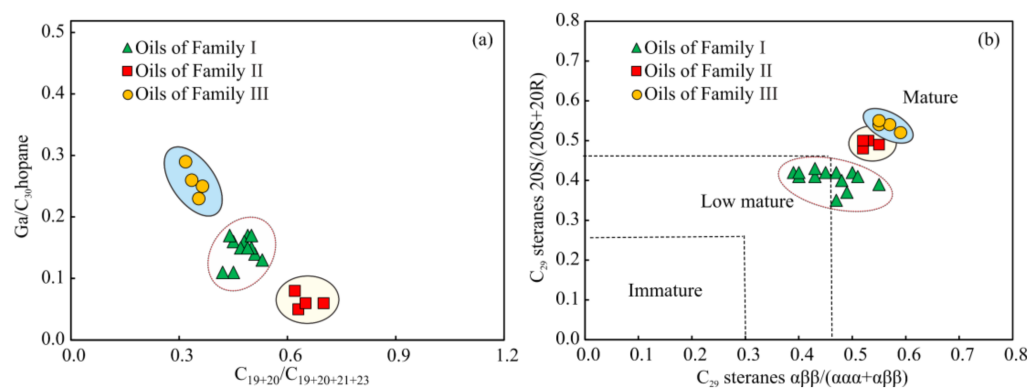


Figure 6. Cross plots of $C_{19+20}/C_{19+20+21+23}$ versus Ga/C_{30} hopane (a) and C_{29} steranes $\alpha\beta/(\alpha\alpha + \alpha\beta)$ versus C_{29} steranes $20S/(20S + 20R)$ (b) of the oil samples in the Fukang Sag.

5.2. Oil–Source Rock Correlation

5.2.1. Comparison of N-Alkanes

The composition and distribution characteristics of the *n*-alkanes mainly depend on the maturity and type of organic matter. In the case of the same source, the crude oil and source rock have similar *n*-alkanes characteristics [59–62]. The gas chromatogram characteristics of the Family I oil were different from those of the coal-measure mudstone of the Badaowan Formation and mudstone of the Pingdiquan Formation. The results suggested that the source rock of the Family I oil was the lacustrine mudstone of the Xishanyao Formation, the source rock of the Family II oil was the coal-measure mudstone of the Badaowan Formation, and the source rock of the Family III oil was the mudstone of the Pingdiquan Formation.

5.2.2. Correlogram Correlation of the Biomarker Parameters

The intersection diagram of the Pr/Ph versus $C_{24}TeT/C_{26}TT$ and the $Ts/(Ts + Tm)$ versus Ga/C_{30} -hopane jointly indicated that the oil samples of the Family I derived from the lacustrine mudstone of the Xishanyao Formation, the oil samples of Family II came from the typical coal-measure mudstone of the Badaowan Formation, and the oil samples of Family III originated from the mudstone of the Pingdiquan Formation. This also further supports the above conclusions (Figure 7).

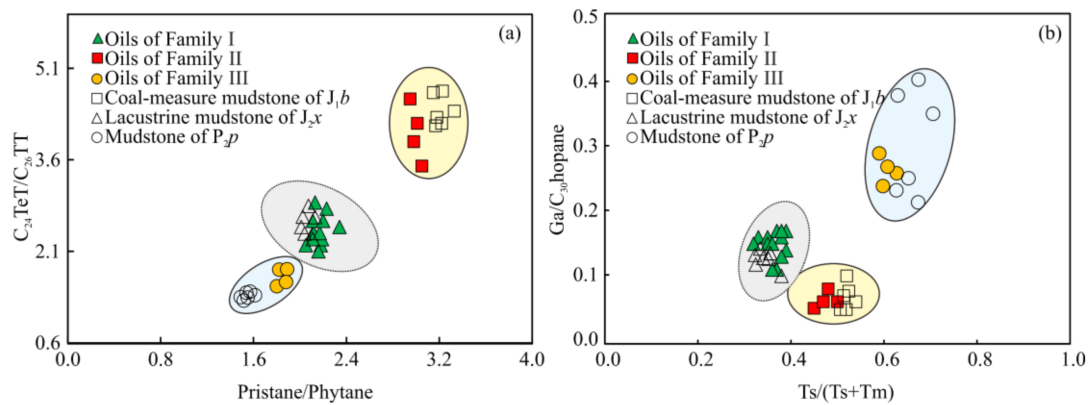


Figure 7. The cross plots of the pristane/phytane versus $C_{24}TeT/C_{26}TT$ (a) and the $Ts/(Ts + Tm)$ versus $Ga/C_{30}hopane$ (b) show the oil–source correlation.

5.2.3. Comparison of the Carbon isotopes $\delta^{13}C$

The carbon isotope composition of the kerogen in Jurassic source rocks is relatively heavy as a whole, in which the isotope value of the Badaowan Formation was $-25.0\text{‰} \sim -28.0\text{‰}$, and that of the Xishanyao Formation was $-26.0\text{‰} \sim -29.0\text{‰}$. However, the carbon isotope value of the Permian Pingdiqian Formation was relatively light, mainly concentrated at $-27.0\text{‰} \sim -32.0\text{‰}$. The mid-range of the $\delta^{13}C$ ratios of the Family I oil ranged between -27.5‰ and -26.8‰ ; they were related to the lacustrine mudstone of the Xishanyao Formation. The $\delta^{13}C$ values of the Family II oil samples varied from $-26.5\text{‰} \sim -26.1\text{‰}$, showing good affinity with the $\delta^{13}C$ of the coal-measure mudstone of the Badaowan Formation. The crude oils of the Family III had light $\delta^{13}C$ values, which indicated that the oils had the same characteristics as the mudstone of the Pingdiqian Formation (Figure 8).

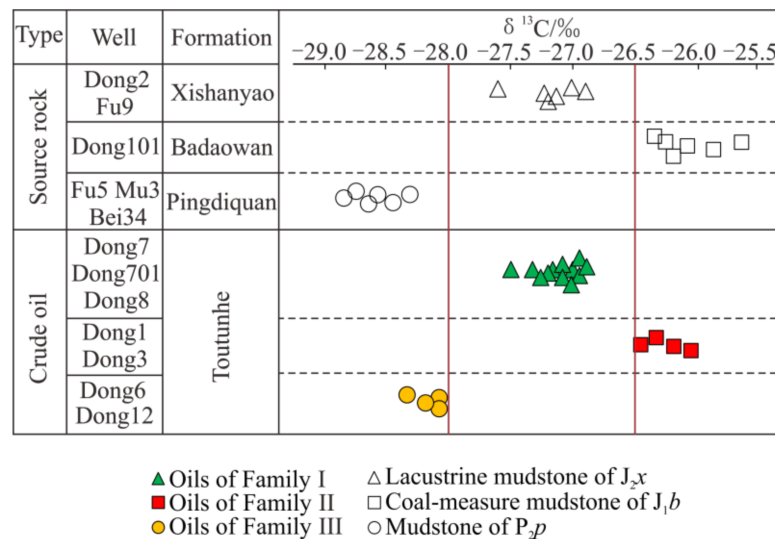


Figure 8. Distribution of the source rock and crude oil of the carbon isotope in Fukang Sag.

6. Conclusions

1. The organic matter abundance of the source rocks in the Fukang Sag was ranked from high to low: Pingdiqian Formation (good quality), Badaowan Formation (fair–good quality), and Xishanyao Formation (fair quality). All samples reached the peak of the oil window based on their geochemical maturity parameters.
2. The crude oil from Fukang Sag can be distinguished as Family I, Family II, and Family III by the differences in the geochemical features. The descending order of crude oil maturity was Family III, Family II, and Family I. The biomarkers and carbon isotopes showed that the Family I oil was derived from the lacustrine mudstone of the

Xishanyao Formation. The Family II oil showed close correlations to the coal-measure mudstone of the Badaowan Formation. The Family III oil was chiefly contributed by mudstone from the Pingdiquan Formation.

3. According to the maturity of the source rocks and crude oil, well locating and exploration in the Fukang Sag of the Junggar Basin can be concentrated in wells with high maturity in the future, and it is recommended that oil and gas be deployed near the Fukang fault zone.

Author Contributions: B.L.: Formal analysis, Writing—review & editing; Y.T.: Methodology, Project administration; Z.C.: Methodology, Supervision; Y.W.: Resources, Validation; D.H.: Writing—review & editing, Project administration; K.Y.: Investigation, Formal analysis; L.C.: Resources, Supervision. All authors have read and agreed to the published version of the manuscript.

Funding: This study was supported by the PetroChina Science and Technology Project (2021DJ0603), the General project of the National Natural Science Foundation of China (No.41972148), and the Open Fund of Collaborative Innovation Center for Unconventional Oil and Gas (Yangtze University) (No.UOG2020-12).

Data Availability Statement: The data used to support the findings of this study are included within the article.

Acknowledgments: The authors are grateful to the Sinopec Shengli Oilfield for their generous donation of samples and additional information.

Conflicts of Interest: The authors declare no competing financial interest.

References

1. Moldowan, J.M.; Seifert, W.K.; Seifert, E.J. Relationship between petroleum composition and depositional environment of petroleum source rocks. *AAPG Bull.* **1985**, *69*, 1255–1268.
2. Huang, H.P.; Zhang, S.C.; Gu, Y.; Su, J. Impacts of source input and secondary alteration on the extended tricyclic terpane ratio: A case study from Palaeozoic sourced oils and condensates in the Tarim Basin, NW China—ScienceDirect. *Org. Geochem.* **2017**, *112*, 158–169. [[CrossRef](#)]
3. Schoell, M. Recent advances in petroleum isotope geochemistry. *Org. Geochem.* **1984**, *6*, 645–663. [[CrossRef](#)]
4. Si, W.; Hou, D.J.; Wu, P.; Zhao, Z.; Ma, X.X.; Zhou, H.F.; Cao, L.Z. Geochemical characteristics of lower cretaceous lacustrine organic matter in the southern sag of the Wuliyasitai depression, Erlian Basin, China. *Mar. Pet. Geol.* **2020**, *118*, 104404. [[CrossRef](#)]
5. Curiale, J.A. Oil–source rock correlations—Limitations and recommendations. *Org. Geochem.* **2008**, *39*, 1150–1161. [[CrossRef](#)]
6. Andrushevich, V.; Engel, M.; Zumberge, J.; Brothers, L. Secular, episodic changes in stable carbon isotope composition of crude oils. *Chem. Geol.* **1998**, *152*, 59–72. [[CrossRef](#)]
7. Mahmoud, L.; Ahmed, A.; Ali, F.; Andrea, M. Organic geochemistry and oil-source rock correlation of the Cretaceous succession in West Wadi El-Rayan (WWER) concession: Implications for a new Cretaceous petroleum system in the north Western Desert, Egypt. *J. Pet. Sci. Eng.* **2022**, *219*, 111071.
8. Xu, W.; Zheng, G.D.; Ma, X.X.; Fortin, D.; Fu, C.C.; Li, Q.; Chelnokov, G.A.; Ershov, V. Chemical and isotopic features of seepage gas from mud volcanoes in southern margin of the Junggar Basin, NW China. *Appl. Geochem.* **2022**, *136*, 105145. [[CrossRef](#)]
9. Tang, Y.J.; Zhang, J.Z.; Li, M.J.; Liu, Y.; Li, M.R.; Sun, P. Origin of crude oils from the paleogene Xingouzu formation in the Jiangling depression of Jiangnan basin, central China. *J. Pet. Sci. Eng.* **2020**, *195*, 107976. [[CrossRef](#)]
10. Cai, C.F.; Zhang, C.M.; Worden, R.H.; Wang, T.K.; Li, H.X.; Jiang, L.; Huang, S.Y.; Zhang, B.S. Application of sulfur and carbon isotopes to oil–source rock correlation: A case study from the Tazhong area, Tarim Basin, China. *Org. Geochem.* **2015**, *83*, 140–152. [[CrossRef](#)]
11. Peters, K.E.; Clark, M.E.; Das Gupta, U.; McCaffrey, M.A.; Lee, C.Y. Recognition of an Infracambrian source rock based on biomarkers in the Baghewala-1 oil, India. *AAPG Bull.* **1995**, *79*, 1481–1493.
12. Peters, K.E. Petroleum tricyclic terpanes: Predicted physicochemical behavior from molecular mechanics calculations. *Org. Geochem.* **2000**, *31*, 497–507. [[CrossRef](#)]
13. Aurea, Y.G.-B.; Eduardo, G.-P.; Luis, M.; Sandra, V.; Fernando, N.-U.; Daniel, G.-R. Deep diagenesis of the Pimienta Formation (Tithonian-Berriasian): Petrophysical, petrographic, and geochemical characteristics of the source rock. *Appl. Geochem.* **2022**, *140*, 105290.
14. Majid, S.F.; Mohammad, R.K.; Hossain, R.; Thomas, G.; Bo, L.; Mehdi, O. Organic geochemistry, oil-source rock, and oil-oil correlation study in a major oilfield in the Middle East. *J. Pet. Sci. Eng.* **2021**, *207*, 109074.
15. Pan, S.; Jiang, Z.; Zhang, Y.; Yuan, X.; Liao, Y. Geochemical characteristics of the lower cretaceous Xiguayuan Formation mudrocks in the Luanping Basin, northern China: Implications for the hydrocarbon generation potential and sedimentary environments. *Mar. Pet. Geol.* **2021**, *133*, 105256. [[CrossRef](#)]

16. Chen, D.; Pang, X.Q.; Li, L.; Jiang, F.J.; Liu, G.Y.; Li, M.; Pang, B.; Jiang, H.; Xu, Z.; Han, W.Y. Organic geochemical characteristics and shale oil potential of the middle Eocene early-mature shale in the Nanpu Sag, Bohai Bay Basin, Eastern China. *Mar. Pet. Geol.* **2021**, *133*, 105248. [[CrossRef](#)]
17. Zhang, Z.D.; Gu, Y.L.; Jin, J.; Li, E.T.; Yu, S.; Pan, C.C. Assessing source and maturity of oils in the Mahu sag, Junggar Basin: Molecular concentrations, compositions and carbon isotopes. *Mar. Pet. Geol.* **2022**, *141*, 105724. [[CrossRef](#)]
18. Wu, Y.P.; Liu, C.L.; Jiang, F.J.; Hu, T.; Lv, J.H.; Zhang, C.X.; Guo, X.G.; Huang, L.L.; Hu, M.L.; Huang, R.D.; et al. Geological characteristics and shale oil potential of alkaline lacustrine source rock in Fengcheng Formation of the Mahu Sag, Junggar Basin, Western China. *J. Pet. Sci. Eng.* **2022**, *216*, 110823. [[CrossRef](#)]
19. Chen, G.Q.; Wang, D.Y.; Yang, F.; Tang, Y.; Zou, X.L.; Ma, W.Y.; Li, M.H. Organic geochemistry and controlling factors of alkaline source rocks within sequence stratigraphic framework in the Fengcheng Formation, Mahu sag, Junggar Basin, NW China. *Energy Explor. Exploit.* **2022**, *40*, 121–142. [[CrossRef](#)]
20. Li, Y.; Lu, J.G.; Liu, X.J.; Wang, J.; Chen, S.J.; He, Q.B. Geochemical characteristics of source rocks and gas exploration direction in Shawan Sag, Junggar Basin. *Nat. Gas Geosci.* **2022**, *33*, 1319–1331. [[CrossRef](#)]
21. Zhu, M.; Liang, Z.L.; Ma, J.; Pang, Z.C.; Wang, J.; Jiao, Y. Patterns of hydrocarbon generation and reservoir distribution in the Jurassic strata, Sikeshu Sag Junggar Basin. *Nat. Gas Geosci.* **2020**, *31*, 488–497.
22. Liu, D.Z. Division of dynamic subsystem for hydrocarbon migration and accumulation in Jurassic middle 4 Block of Jungar Basin and its exploration significance. *Fault Block Oil Gas Field* **2020**, *27*, 149–154.
23. He, H.Q.; Zhi, D.M.; Tang, Y.; Liu, C.W.; Chen, H.; Guo, X.G.; Wang, Z.S. A great discovery of Well Kangtan 1 in the Fukang Sag in the Junggar Basin and its significance. *China Pet. Explor.* **2021**, *26*, 1–11.
24. Gao, G.; Titi, A.; Yang, S.R.; Tang, Y.; Kong, Y.H.; He, W.J. Geochemistry and depositional environment of fresh lacustrine source rock: A case study from the Triassic Baijiantan Formation shales in Junggar Basin, northwest China. *Org. Geochem.* **2017**, *113*, 75–89. [[CrossRef](#)]
25. Tao, K.Y.; Cao, J.; Wang, Y.C.; Ma, W.Y.; Xiang, B.L.; Ren, J.L.; Zhou, N. Geochemistry and origin of natural gas in the petroliferous Mahu sag, northwestern Junggar Basin, NW China: Carboniferous marine and Permian lacustrine gas systems. *Org. Geochem.* **2016**, *100*, 62–79. [[CrossRef](#)]
26. Sun, F.N.; Hu, W.X.; Zhang, Z.R.; Cao, J. Isotopic evidence for the formation of 25-norhopanes via in situ biodegradation in the Permian Lucaogou shales, southern Junggar Basin. *Org. Geochem.* **2022**, *163*, 104334. [[CrossRef](#)]
27. Zhou, L.; Pang, X.; Wu, L.; Kuang, L.; Jiang, F.; Pang, H.; Peng, J.; Yu, R. Critical conditions for tight oil charging and delineation of effective oil source rocks in Lucaogou Formation, Jimusar Sag, Junggar Basin, northwest China. *Aust. J. Earth Sci.* **2016**, *63*, 205–216. [[CrossRef](#)]
28. Zheng, M.L.; Tian, A.J.; Yang, T.Y.; He, W.J.; Chen, L.; Wu, H.S.; Ding, J. Structural evolution and hydrocarbon accumulation in the eastern Junggar Basin. *Oil Gas Geol.* **2018**, *39*, 907–917.
29. Wang, X.J.; Song, Y.; Zheng, M.L.; Ren, H.J.; Wu, H.S.; He, W.J.; Wang, T.; Wang, X.T.; ZHao, C.Y.; Guo, J.C. Composite petroleum system and multi-stage hydrocarbon accumulation in Junggar Basin. *China Pet. Explor.* **2021**, *26*, 29–43.
30. Liu, H.L.; Li, H.; Xiang, H.; Wang, X.Y.; Du, S.K. Geochemistry, genesis and distribution of crude oils in the Fukang fault zones and their periphery in Junggar Basin. *Oil. Gas. Geol.* **2020**, *31*, 258–267.
31. Chen, J.P.; Wang, X.L.; Deng, C.P.; Liang, D.G.; Zhang, Y.Q.; Zhao, Z.; Ni, Y.Y.; Zhi, D.M.; Yang, H.B.; Wang, Y.T. Oil and gas source, occurrence and petroleum system in the Junggar Basin, Northwest China. *Acta Geol. Sin.* **2016**, *90*, 421–450.
32. Chen, J.P.; Deng, C.P.; Liang, D.G.; Wang, X.L.; Song, F.Q.; Xue, X.K.; Jin, T.; Zhong, N.N. Quantification of mixed oil derived from multiple source rocks: a typical case study of the Cainan Oilfield in the East Junggar Basin, Northwest China. *Acta Geol. Sin.* **2004**, *78*, 279–288.
33. Carroll, A.R.; Liang, Y.; Graham, S.A.; Xiao, X.; Hendrix, M.S.; Chu, J.; Mcknight, C.L. Junggar basin, northwest China: Trapped Late Paleozoic ocean. *Tectonophysics* **1990**, *181*, 1–14. [[CrossRef](#)]
34. Carroll, A.R. Upper Permian lacustrine organic facies evolution, Southern Junggar Basin, NW China. *Org. Geochem.* **1998**, *28*, 649–667. [[CrossRef](#)]
35. Liu, G.D.; Chen, Z.L.; Wang, X.L.; Gao, G.; Xiang, B.L.; Ren, J.L.; Ma, W.Y. Migration and accumulation of crude oils from Permian lacustrine source rocks to Triassic reservoirs in the Mahu depression of Junggar Basin, NW China: Constraints from pyrrolic nitrogen compounds and fluid inclusion analysis. *Org. Geochem.* **2016**, *101*, 82–98. [[CrossRef](#)]
36. Wang, Y.Z.; Lin, M.R.; Xi, K.L.; Cao, Y.C.; Wang, J.; Yuan, G.H.; Kashif, M.; Song, M.S. Characteristics and origin of the major authigenic minerals and their impacts on reservoir quality in the Permian Wutonggou Formation of Fukang Sag, Junggar Basin, western China. *Mar. Pet. Geol.* **2018**, *97*, 241–259. [[CrossRef](#)]
37. Cao, B.F.; Luo, X.R.; Zhang, L.K.; Sui, F.G.; Lin, H.X.; Lei, Y.H. Diagenetic evolution of deep sandstones and multiple-stage oil entrapment: A case study from the Lower Jurassic Sangonghe Formation in the Fukang Sag, central Junggar Basin (NW China). *J. Pet. Sci. Eng.* **2017**, *152*, 136–155. [[CrossRef](#)]
38. Yu, Z.C.; Wang, Z.Z.; Fan, W.T.; Wang, J.; Li, Z.Y. Evaluating the sedimentological and diagenetic impacts on terrestrial lacustrine fan delta sandy conglomerates reservoir quality: Insights from the Triassic Baikouquan Formation in the Mahu sag, Junggar Basin, Western China. *Mar. Pet. Geol.* **2022**, *146*, 105973. [[CrossRef](#)]

39. Cao, B.F.; Luo, X.R.; Zhang, L.K.; Sui, F.G.; Lin, H.X.; Lei, Y.H. Diagenetic Heterogeneity of Deep Sandstones and Its Relationship to Oil Emplacement: A Case Study from the Middle Jurassic Toutunhe Formation in the Fukang Sag, Central Junggar Basin (NW China). *Geofluids* **2017**, *2017*, 4292079. [[CrossRef](#)]
40. Fang, S.H.; Guo, Z.J.; Song, Y.; Wu, C.D.; Fan, R.D. Sedimentary facies evolution and basin pattern of the Jurassic in southern margin area of Junggar Basin. *J. Palaeogeogr.* **2005**, *7*, 347–356.
41. Zhao, X.Z.; Zhou, L.H.; Pu, X.G.; Jiang, W.Y.; Jin, F.M.; Xiao, D.Q.; Han, W.Z.; Zhang, W.; Shi, Z.N.; Li, Y. Hydrocarbon Generating Potential of the Upper Paleozoic Section of the Huanghua Depression, Bohai Bay Basin, China. *Energy Fuels* **2018**, *32*, 12351–12364. [[CrossRef](#)]
42. Li, B.C.; He, D.X.; Li, M.J.; Chen, L.; Yan, K.; Tang, Y.J. Biomarkers and Carbon Isotope of Monomer Hydrocarbon in Application for Oil–Source Correlation and Migration in the Moxizhuang–Yongjin Block, Junggar Basin, NW China. *ACS Omega* **2022**, *7*, 47317–47329. [[CrossRef](#)] [[PubMed](#)]
43. Li, Y.; Wang, Z.S.; Wu, P.; Gao, X.D.; Yu, Z.L.; Yu, Y.; Yang, J.H. Organic geochemistry of Upper Paleozoic source rocks in the eastern margin of the Ordos Basin, China: Input and hydrocarbon generation potential. *J. Pet. Sci. Eng.* **2019**, *181*, 106202. [[CrossRef](#)]
44. Espitalié, J.; Bordenave, M.L. *Rock-Eval Pyrolysis*; Editions Technip: Paris, France, 1993; pp. 237–272.
45. Chai, Z.; Chen, Z.H. Biomarkers, light hydrocarbons, and diamondoids of petroleum in deep reservoirs of the southeast Tabei Uplift, Tarim Basin: Implication for its origin, alteration, and charging direction. *Mar. Pet. Geol.* **2022**, *147*, 106019. [[CrossRef](#)]
46. Lu, X.L.; Li, M.J.; Wang, X.J.; Wei, T.Q.; Tang, Y.J.; Hong, H.T.; Wu, C.J.; Yang, X.; Liu, Y. Distribution and Geochemical Significance of Rearranged Hopanes in Jurassic Source Rocks and Related Oils in the Center of the Sichuan Basin, China. *ACS Omega* **2021**, *6*, 100252. [[CrossRef](#)]
47. Espitalié, J.; Laporte, J.L.; Madec, M.; Marquis, F.; Leplat, P.; Paulet, J.; Boutefeu, A. Méthode rapide de caractérisation des roches mères, de leur potentiel pétrolier et de leur degré d'évolution. *Rev. Inst. Fr. Pet.* **1977**, *32*, 23–42. [[CrossRef](#)]
48. Xiao, H.; Wang, T.G.; Li, M.J.; Chen, D.X.; Chang, J.; Song, D.F.; Yang, C.Y.; Hu, Y.J.; Ali, S. Oil sources and accumulation processes of the Neoproterozoic Luotuoling Formation reservoirs (~930 Ma) in North China Craton. *J. Pet. Sci. Eng.* **2022**, *211*, 110186. [[CrossRef](#)]
49. Farrimond, P.; Bevan, J.C.; Bishop, A.N. Tricyclic terpane maturity parameters: Response to heating by an igneous intrusion. *Org. Geochem.* **1999**, *30*, 1011–1019. [[CrossRef](#)]
50. Graas, G.W.V. Biomarker maturity parameters for high maturities: Calibration of the working range up to the oil/condensate threshold. *Org. Geochem.* **1990**, *16*, 1025–1032. [[CrossRef](#)]
51. Grande, S.M.B.D.; Neto, F.R.A.M.; Mello, M.R. Extended tricyclic terpanes in sediments and petroleum. *Org. Geochem.* **1993**, *20*, 1039–1047. [[CrossRef](#)]
52. Ourisson, G.; Albrecht, P.; Rohmer, M. Predictive microbial biochemistry—From molecular fossils to procaryotic membranes. *Trends Biochem. Sci.* **1982**, *7*, 236–239. [[CrossRef](#)]
53. Tao, S.Z.; Wang, C.Y.; Du, J.G.; Liu, L.; Chen, Z. Geochemical application of tricyclic and tetracyclic terpanes biomarkers in crude oils of NW China. *Mar. Pet. Geol.* **2015**, *67*, 460–467. [[CrossRef](#)]
54. Powell, T.G.; McKirdy, D.M. Relationship between ratio of pristane to phytane, crude oil composition and geological environment in Australia. *Nat. Phys. Sci.* **1973**, *243*, 37–39. [[CrossRef](#)]
55. Didyk, B.M.; Simoneit, B.R.T.; Brassell, S.C.T.; Eglinton, G. Organic geochemical indicators of palaeoenvironmental conditions of sedimentation. *Nature* **1978**, *272*, 216–222. [[CrossRef](#)]
56. Peters, K.E.; Walters, C.C.; Moldowan, J.M. *Biomarkers and Isotopes in Petroleum Exploration and Earth History*; Cambridge University Press: Cambridge, UK, 2005; pp. 9–168.
57. Seifert, W.K.; Moldowan, J.M. Applications of steranes, terpanes and monoaromatics to the maturation, migration and source of crude oils. *Geochim. Cosmochim. Acta* **1978**, *42*, 77–95. [[CrossRef](#)]
58. Chang, X.C.; Shi, B.B.; Liu, Z.Q.; Wang, Y.; Xu, Y.D. Investigation on the biodegradation levels of super heavy oils by parameter-stripping method and refined Manco scale: A case study from the Chepaizi Uplift of Junggar Basin. *Pet. Sci.* **2021**, *18*, 380–397. [[CrossRef](#)]
59. Volk, H.; George, S.C.; Middleton, H.; Schofield, S. Geochemical comparison of fluid inclusion and present-day oil accumulations in the Papuan Foreland—evidence for previously unrecognised petroleum source rocks. *Org. Geochem.* **2005**, *36*, 29–51. [[CrossRef](#)]
60. Volkman, J.K. A review of sterol markers for marine and terrigenous organic matter. *Org. Geochem.* **1986**, *9*, 83–99. [[CrossRef](#)]
61. Zhang, Y.J.; Hong, L.; Wang, Y.P.; Xin, Z.; Peng, P.A. Organic geochemical characteristics of Eocene crude oils from Zhanhua Depression, Bohai Bay Basin, China. *Acta Geochim.* **2020**, *39*, 655–667. [[CrossRef](#)]
62. Körmös, S.; Sachsenhofer, R.F.; Bechtel, A.; Radovics, B.G.; Milota, K.; Schubert, F. Source rock potential, crude oil characteristics and oil-to-source rock correlation in a Central Paratethys sub-basin, the Hungarian Palaeogene Basin (Pannonian Basin). *Mar. Pet. Geol.* **2021**, *127*, 104955. [[CrossRef](#)]

Disclaimer/Publisher's Note: The statements, opinions and data contained in all publications are solely those of the individual author(s) and contributor(s) and not of MDPI and/or the editor(s). MDPI and/or the editor(s) disclaim responsibility for any injury to people or property resulting from any ideas, methods, instructions or products referred to in the content.